Available online at www.sciencedirect.com
ScienceDirect
Biochemical and Biophysical Research Communications 362 (2007) 766–772
BBRC
www.elsevier.com/locate/ybbrc

Inducing rigid local structure around the zinc-binding region by hydrophobic interactions enhances the homotrimerization and apoptotic activity of zinc-free TRAIL

Hyun-Wook Lee [a], Tae-In Kim [b], Khon Huynh Chan [a], Myung-Hee Kwon [b], Jeong-Sun Kim [c], Moonsoo Jin [d], Yong-Sung Kim [a,*]

[a] *Department of Molecular Science and Technology, Ajou University, San5, Wonchon-dong, Yeongtong-gu, Suwon 443-749, Republic of Korea*
[b] *Department of Microbiology, Ajou University School of Medicine, Suwon 443-721, Republic of Korea*
[c] *Department of Chemistry, Chonnam National University, Gwangju 500-757, Republic of Korea*
[d] *Department of Biomedical Engineering, Cornell University, Ithaca, NY 14853, USA*

Received 8 August 2007
Available online 24 August 2007

Abstract

Tumor necrosis factor-related apoptosis-inducing ligand (TRAIL), existing as homotrimer in solution, contains a unique zinc-binding site coordinated by three Cys230 residues at the tip of trimeric interface. TRAIL mutant with replacements of Cys230 with Ala ($TRAIL_{C230A}$) negligibly formed trimeric structure and showed no apoptotic activity. Here, to elucidate the relationship between the trimeric stability and the apoptotic activity of $TRAIL_{C230A}$, we rationally designed mutations to induce homotrimerization of $TRAIL_{C230A}$ by substituting for the three residues involved in hydrogen bonding (Tyr183 and Tyr243) and putative repulsive electrostatic (Arg227) interactions at the buried trimeric interface into hydrophobic residues, like Y183F, Y243F, and R227I. The $TRAIL_{C230A}$-derived mutants exhibited enhanced homotrimerization, but only the mutants containing R227I exhibited significant apoptosis-inducing activity in cancer cells. These results, together with the induction of rigid local structure around the zinc-binding region by R227I in $TRAIL_{C230A}$, suggest that ordered, rigid structure around the zinc-binding region is critical for the homotrimerization and apoptotic activity of TRAIL.

Keywords: TRAIL; Zinc-free TRAIL; Trimeric stability; Apoptosis; Zinc ion; Cys230

Tumor necrosis factor (TNF)-related apoptosis-inducing ligand (TRAIL) is an attractive anti-cancer agent because it can induce apoptotic cell death in a variety of tumor cells without significant cytotoxicity on normal cells *in vitro* and *in vivo* [1–4]. TRAIL can specifically interact with five distinct receptors, two of which are death receptors (DR4/TRAIL-R1 (TR1) and DR5/TRAIL-R2 (TR2)) [1,2]. TRAIL binding to TR1 or TR2 results in conformational changes of the receptor that subsequently transmit cell death signaling through the receptor's intracellular death domain [1,2]. Like other TNF family ligands, TRAIL (residues 114–281), composed entirely of two antiparallel β-pleated sheets and loops in a standard jellyroll topology, interacts with the adjacent subunits in a head-to-tail fashion to form a wedge-shaped homotrimer in solution [5,6]. The 3:3 complex structure of TRAIL-TR2, where three TR2 molecules interact diagonally with the interfaces between each subunit of TRAIL trimer, suggests that the homotrimer formation of TRAIL is essential for inducing receptor clustering and subsequent cell death signaling [7,8].

Each TRAIL monomer contains one unpaired cysteine at position 230, Cys230. The three Cys230 residues from each subunit are closely located one another at the three-fold symmetric axis near the tip of wedge-shaped homotrimer

* Corresponding author. Fax: +82 31 219 1610.
E-mail address: kimys@ajou.ac.kr (Y.-S. Kim).

0006-291X/$ - see front matter © 2007 Elsevier Inc. All rights reserved.
doi:10.1016/j.bbrc.2007.08.075

[5,6]. The buried Cys230 residues coordinate a zinc ion (Zn^{2+}) in conjunction with a chloride ion, resulting in a unique tetrahedral zinc-binding site in TRAIL trimer [6]. Numerous studies of TRAIL with substitutions of Cys230 with other residues of Ala, Ser or Gly resulted in significant loss of the quaternary structure and the bioactivity of inducing apoptotic cell death [6,9–11]. Further, zinc-depleted TRAIL has lower thermodynamic stability and solubility to be easily converted into biologically inactive dimeric and/or monomeric forms and aggregated species [5–7,9,10]. These results demonstrate that zinc coordination by Cys230 is essential for maintaining the structure and stability, and, hence, the biological activity of TRAIL. However, why zinc-depleted or Cys230-substituted TRAIL mutants lose the trimeric stability and apoptosis-inducing activity has been poorly understood.

The aim of this study is to elucidate the relationship between the trimeric stability and the apoptotic activity of Cys230-substituted TRAIL mutant (designated as 'zinc-free TRAIL'). For this, we rationally designed mutations to induce homotrimerization of TRAIL C230A mutant ($TRAIL_{C230A}$) by replacing the three residues involved in hydrogen bonding (Tyr183 and Tyr243) and putative repulsive electrostatic (Arg227) interactions at the threefold symmetric axis of TRAIL with hydrophobic residues, like Y183F, Y243F, and R227I, which would promote hydrophobic contacts at the trimeric interface. We found that, even though $TRAIL_{C230A}$-derived mutants exhibited enhanced homotrimerization, only the mutants containing R227I showed significant apoptotic activities in cancer cells. R227I, located near the zinc-binding site, induced rigid local structure around the zinc-binding region of $TRAIL_{C230A}$-derived mutants. Our results provide some insights why zinc-free TRAIL loses the trimeric stability and apoptosis-inducing activity.

Materials and methods

Site-directed mutagenesis. The bacterial expression plasmid pETd-wHisTRAIL, encoding soluble TRAIL (residues 114–281 with N-terminal 6× His-tag), was described before [4,12]. Single-site substitution for generating TRAIL mutants was performed by site-directed mutagenesis [13]. Oligonucleotides were synthesized from Bioneer Co. (Korea). All the constructs were confirmed by sequencing (GenoTech, Korea).

Bacterial expression and purification of wild-type TRAIL and mutants. Wild-type TRAIL and mutants (residues 114–281 with a N-terminal 6× His-tag) were expressed in the cytosol of *Escherichia coli* BL21(DE3) strain and then purified using anti-His Talon resin (Clontech), as previously described [4,12]. Particularly, during the expression of wild-type TRAIL and its derived mutants in *E. coli*, 100 μM $ZnSO_4$ was supplemented to the LB medium to ensure that they contain zinc ion [6]. Purified proteins were greater than 95% pure as assayed by SDS–PAGE. Protein concentrations were determined using the Bio-Rad protein assay kit. The purified proteins were sterilized by filtration using a cellulose acetate membrane filter (0.2 μm) (Nalgene Co.) for cell-based assays.

Size exclusion chromatography (SEC). SEC analyses were performed on a Agilent 1100 high performance liquid chromatography system using Superdex 200 GL size-exclusion column (10 × 300 mm, GE Healthcare), with a mobile phase of 13 mM sodium phosphate, pH 6.5, plus 400 mM ammonium sulfate ($(NH_4)_2SO_4$) at a flow rate of 0.5 ml/min [3,13]. The purified proteins (10 μM) were subjected to the SEC analyses in a volume of 100 μl. Chromatograms were obtained by monitoring absorbance at 280 nm. Apparent molecular weight (MW) samples were estimated by fitting elution volume into the calibration curve of the MW standards (Amersham Bioscience).

Biological activity of wild-type TRAIL and mutants in vitro. Adherent HCT116 cells were maintained in DMEM supplemented with 10% fetal calf serum, 100 U/ml penicillin, and 100 μg/ml streptomycin (Gibco Invitrogen) [4]. The cells were seeded at density of 1×10^4 cells/well in 96-well plate, cultured overnight, and then incubated for 24 h with wild-type TRAIL and mutants at varying concentrations. Cell viability was analyzed using a colorimetric MTT (3-(4,5-dimethylthiazol-2-yl)-2,5-diphenyltetrazolium bromide)-based Cell Growth Determination kit (Sigma) [4]. The EC_{50} value (effective concentration for 50% cell death) was calculated by complex sigmoid non-linear regression analysis using Sigma plot software (SPSS Inc.).

Fluorescence spectroscopy. Intrinsic tryptophan fluorescence emission spectra were recorded at 25 °C in a FP-6500 spectrofluorometer (Jasco Inc.). Spectra were obtained by using 1 μM protein solutions in a buffer (13 mM sodium phosphate, pH 6.5, plus 400 mM ammonium sulfate ($(NH_4)_2SO_4$)) and rectangular quartz cells having a path length of 1 cm. Excitation wavelength was at 295 nm, and the emission spectrum was scanned from 305 to 400 nm using 0.5-nm step size and a 1 s integration time [6].

Results

Residue identification to induce homotrimerization of $TRAIL_{C230A}$

C230A-substituted TRAIL, $TRAIL_{C230A}$, was used as a template to design zinc-free TRAIL variants that do not require zinc ion to form the homotrimeric complex and to exert the biological activity. Previously thermodynamically stable wild-type TRAIL variants were designed by replacing some residues in the monomeric subunit or at dimeric interfaces into energetically favorable residues [14]. The strategy we have taken here was replacing the residues involved in energetically unfavorable interactions at the buried trimeric interfaces with the hydrophobic residues to promote homotrimerization of $TRAIL_{C230A}$. Like other TNF family ligands, TRAIL has nine aromatic residues (Tyr183, Tyr243, and Phe278 from each subunit) at the trimeric interface along the threefold symmetric axis, providing hydrophobic and/or hydrogen bonding interactions between adjacent subunits [5,7,8]. Specifically, the six hydroxyl groups out of Tyr183 and Tyr243 side chains form a hexagonal hydrogen-bonding network, which is vertical to the axis (Fig. 1). However, there is still a large cavity between Tyr183 and Cys230 along the trimeric axis of TRAIL [6,15], indicating that filling the cavity by hydrophobic residues might be a good strategy for inducing homotrimerization of TRAIL [7]. Thus, we first predicted alternative residues replacing Tyr183 and Tyr243 residues into hydrophobic Phe. Interestingly, Tyr183 appears as Phe in other TNF family ligands of TNFβ and FasL [5,7]. Second, the crystal structure showed that the Arg227 side chain adopts two rotamer conformations (Fig. 1), implying the flexibility of the side chain [6]. Furthermore, it is located closely to one another (less than

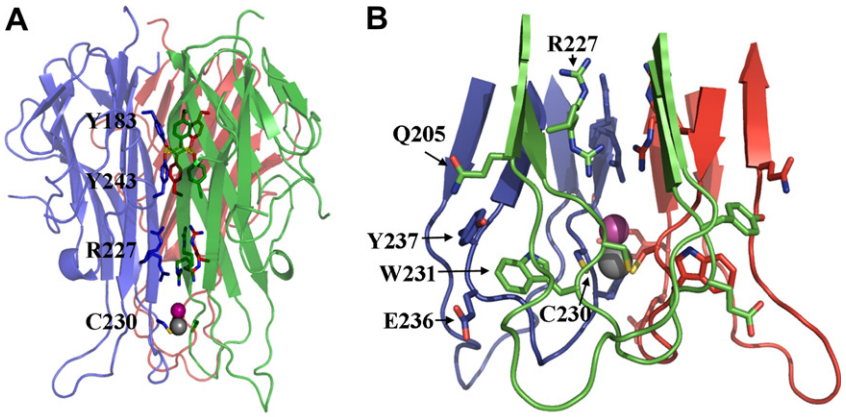

Fig. 1. Structural features of TRAIL highlighting the mutated residues and the zinc-binding region. (A) Side view of homotrimeric TRAIL highlighting the mutated residues (Cys230, Tyr183, Tyr243, and Arg227) in stick model, zinc (grey) and chloride (pink) ions at the zinc-binding site. (B) Detailed view of the zinc-binding region between the residues 227–241. The residues mentioned in the text were highlighted in stick model. In (A) and (B), each subunit of TRAIL is represented in different colors of green, blue, and red. The sulfur, nitrogen, and oxygen atoms are shown as yellow, blue, and red, respectively. The images were generated using PyMol software (DeLano Scientific LLC) based on the trimeric TRAIL structure (PDB code 1D0G) [6].

3 Å) at the trimeric interface, which might invoke charge repulsion among them. Since the positive charges of Arg227 would not be well compensated in the hydrophobic environment [14], we decided to substitute the hydrophobic Ile for Arg227 to abolish, if any, the repulsive electrostatic interactions as well as to create favorable hydrophobic contact.

Construction and purification of TRAIL$_{C230A}$-derived mutants

As shown in Table 1, the three mutations, Y183F, Y243F, and R227I, were introduced alone or in combination into TRAIL$_{C230A}$ by site-directed mutagenesis. For comparisons, the mutations were also introduced sequentially into wild-type TRAIL. His-tagged wild-type TRAIL and mutants were expressed in *E. coli* and purified with more than 95% purity [4,12]. All the proteins, including wild-type TRAIL and TRAIL$_{C230A}$, were solubly expressed well with purification yields of ~0.4 to 1.8 mg out of 1-L shake flask culture, showing mutants with more hydrophobic substitutions less soluble expression levels.

Homotrimerization levels of TRAIL$_{C230A}$-derived mutants

SEC was employed to estimate homotrimer formation of the purified TRAIL mutants in solution under native conditions. Relative tendency to form homotrimer for each

Table 1
Comparisons of TR2 binding affinity, homotrimerization level, and apoptosis-inducing activity between wild-type TRAIL, TRAIL$_{C230A}$ and their mutants[a]

Clones	Mutations	TR2 affinity ratio (mutant/wild-type)[b]	Homotrimerization level (%)[c]	Apoptosis EC_{50} (ng/ml)[d]
Wild-type	—	—	—	20.2 ± 1.8
M1	Y183F	1.7	96.3	26.5 ± 1.2
M2	Y183F, Y243F	1.1	95.5	26.4 ± 1.7
M3	Y183F, Y243F, R227I	1.3	96.0	17.0 ± 1.4
M4	R227I	1.0	94.3	23.6 ± 2.0
TRAIL$_{C230A}$	C230A	4.4	1.8	No activity
M5	C230A, Y183F	3.9	29.5	No activity
M6	C230A, Y243F	6.6	8.0	No activity
M7	C230A, R227I	3.1	70.0	55.4 ± 1.8
M8	C230A, Y183F, Y243F	3.1	41.1	No activity
M9	C230A, Y183F, R227I	7.0	72.4	48.6 ± 2.7
M10	C230A, Y243F, R227I	4.6	75.9	71.6 ± 8.8
M11	C230A, Y183F, Y243F, R227I	6.7	80.4	49.5 ± 3.5

[a] The mutation sites introduced were indicated by the single-letter amino acid code.
[b] The ratio of dissociation constants (K_D) of mutants to wild-type for TR2 binding. The K_D value of wild-type TRAIL for the TR2 binding was 9.9 ± 0.1 nM (Supplementary Table S1). Dissociation (k_{off}) and association (k_{on}) rate constants and K_D values of each mutant were shown in Supplementary Table S1.
[c] The homotrimerization level of TRAIL mutants was represented as percentage by comparing the peak areas for trimeric species obtained from SEC analyses with that of wild-type TRAIL, after injection of the same concentration (10 μM).
[d] Apoptotic cell death inducing activity of wild-type TRAIL and mutants was analyzed on HCT116 cells using MTT assay and the EC_{50} value was calculated by complex sigmoid non-linear regression analysis.

TRAIL mutant, designated as 'homotrimerization level', was calculated as percentage by comparing the peak areas for the trimeric species with that of wild-type TRAIL after injection of the same concentration of 10 μM (Fig. 2 and Table 1). Even though the exact homotrimerization constant is not available for wild-type TRAIL, previous SEC and crystallographic studies have shown that wild-type TRAIL exists as a stable trimer in solution, down to at least micromolar concentrations [5,6,11,12]. As expected, wild-type TRAIL was eluted as a trimer with the expected MW of ~60 kDa (~20 kDa × 3) (Fig. 2A). The wild-type TRAIL-derived mutants (M1–M4) were also eluted as trimeric species without any detectable dimeric, monomeric, or aggregated species. We cannot distinguish the differences in the trimerization tendency between wild-type TRAIL and its derived mutants within the concentration limits of detection for SEC (>2 μM) monitored by absorbance at 280 nm (data not shown).

Injection of $TRAIL_{C230A}$ up to 100 μM did not show any peaks for monomeric, dimeric or trimeric position (Fig. 2B). Changes in elution buffers with different pH and ionic strength or SEC columns with different resins gave the same result (data not shown) [3,11]. A previous report showed that TRAIL mutant with the replacement of Cys230 with Ser, was barely detected as the monomeric form by SEC [9]. There are many aromatic residues at the dimeric and/or trimeric interface of TRAIL [5,6]. Thus, incapability of $TRAIL_{C230A}$ to form the trimeric state could expose the hydrophobic residues into solvent, which might result in adherence to the matrix of the column not to be eluted at all.

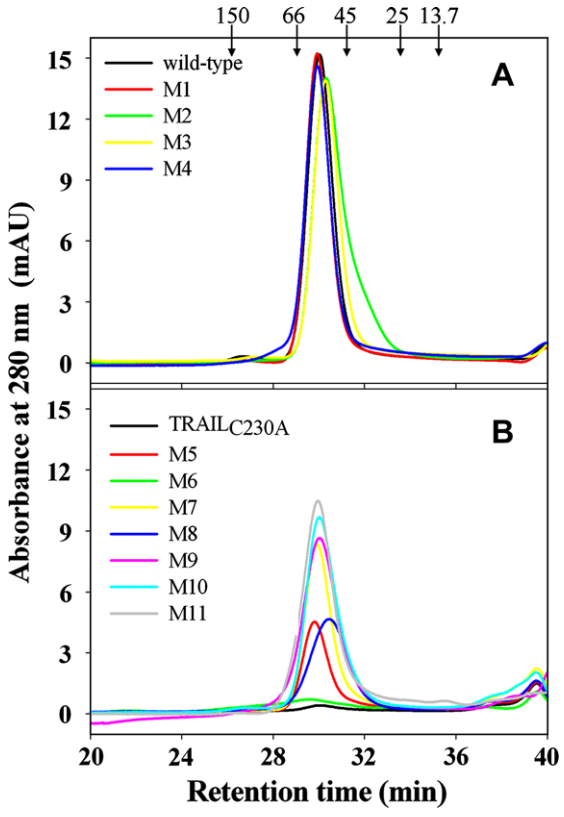

Fig. 2. SEC elution profiles of the purified wild-type TRAIL and its derived mutants (A) and $TRAIL_{C230A}$ and its derived mutants (B). All the proteins were injected at 10 μM and the absorbance was monitored at 280 nm. Each protein was indicated in different colors. Arrows indicate the elution positions of MW standards (alcohol dehydrogenase, 150 kDa; bovine serum albumin, 66 kDa; ovalbumin, 45 kDa; chymotrypsinogen, 25 kDa; ribonuclease A, 13.7 kDa).

The $TRAIL_{C230A}$-derived mutants with substitutions of Y183F, Y243F, and/or R227I alone or in combination showed much dramatic differences in the tendency to form the homotrimer, though the elution positions of which slightly varied depending on the mutations (Fig. 2B). For the single-site substituted mutants, M5 (Y183F), M6 (Y243F), and M7 (R227I) showed ~30%, ~8%, and ~70% homotrimerization level of wild-type TRAIL, respectively, demonstrating that R227I mutation most effectively induced homotrimerization of $TRAIL_{C230A}$ (Table 1). Even M8 containing both Y183F and Y243F showed only ~40% trimerization level. Addition of either Y183F (M9) or Y243F (M10) to M7 (R227I) only slightly augmented the homotrimerization level. Among the $TRAIL_{C230A}$-derived mutants, M11 (Y183F + Y243F + R227I) showed the highest homotrimerization level of ~80%, compared with wild-type TRAIL. All the mutants tested did not show any higher oligomeric species than the trimeric form (Fig. 2B).

Binding and biological activities of $TRAIL_{C230A}$-derived mutants

To characterize effects of introduced mutations on the affinity with a receptor, kinetic binding interactions between TRAIL mutants and TR2 were measured at 25 °C using SPR by flowing the mutants over TR2-immobilized surface (Table 1). The detailed kinetic parameters and sensograms are shown in Supplementary Table S1 and Fig. S1, respectively. The 3:3 complex structure of TRAIL-TR2 displays three TR2s interact diagonally with the exposed intersubunit crevices of homotrimeric TRAIL [7,8,15]. Since all the mutated residues of Cys230, Tyr183, Arg227, and Try243 are located in the buried trimeric interface of TRAIL (Fig. 1), they are not expected to disrupt interactions with the receptor. SPR analysis of TRAIL mutants exhibited no dramatic differences in the affinity with TR2, compared with wild-type TRAIL (Table 1). The dissociation constant (K_D) values ranged between 9 and 18 nM for wild-type TRAIL and its derived mutants (M1–M4) and 40–70 nM for $TRAIL_{C230A}$ and its derived mutants (M5–M11) (Supplementary Table S1). The K_D values for wild-type TRAIL and $TRAIL_{C230A}$ matched well with the previous data [6].

We then assessed biological activity of TRAIL mutants against TRAIL-sensitive HCT116 cancer cells (colorectal carcinoma) with MTT-based viability assay (Fig. 3) [4]. Wild-type TRAIL-derived mutants (M1–M4) exhibited comparable cell death-inducing activities in HCT116 cells

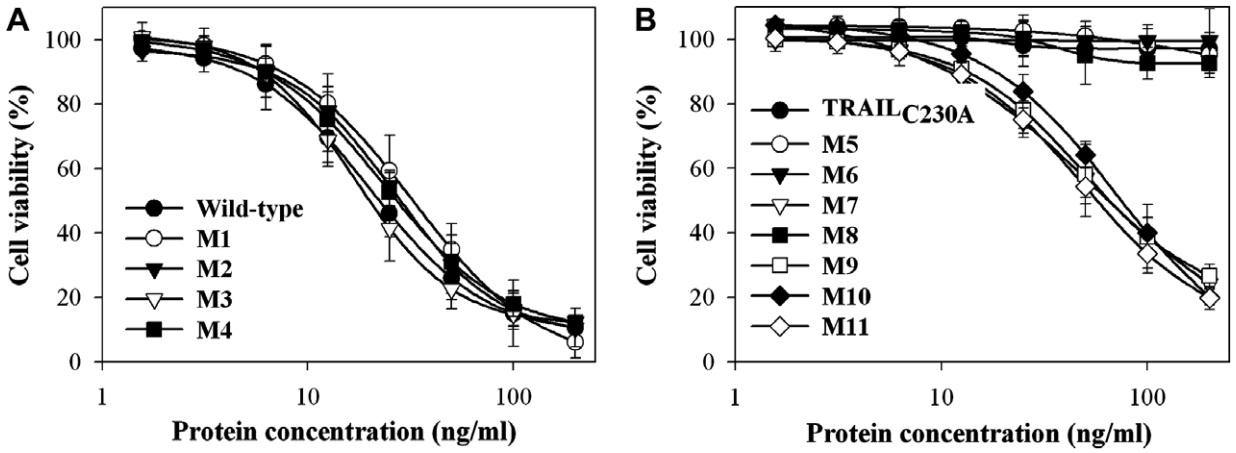

Fig. 3. Cell-death inducing activity of wild-type TRAIL and its derived mutants (A) and $TRAIL_{C230A}$ and its derived mutants (B) on HCT116 cells. Cells were incubated with the indicated concentrations of proteins (1–200 ng/ml) for 24 h. The cell viability was determined by MTT assay and presented as percentage of viable cells compared with untreated, control cells. The solid lines indicate the fitting curve into the data by complex sigmoid non-linear regression analysis on Sigma Plot software. Error bars indicate the standard deviations for at least triplicated experiments.

to that of wild-type TRAIL, which showed ~20 ng/ml of EC_{50} (effective concentration for 50% cell death) (Fig. 3A and Table 1). $TRAIL_{C230A}$ was totally inactive for the cells over the concentrations (5–200 ng/ml) tested for 24 h (Fig. 3B), consistent with previous data for $TRAIL_{C230A}$ in Jurkat cells [9] and $TRAIL_{C230G}$ in HeLa cells [10]. $TRAIL_{C230A}$-derived mutants of M5 (Y183F), M6 (Y243F), and M8 (Y183F + Y243F) did not induce cell death at all in both cells even at the highest concentration (200 ng/ml) for 24 h, although they had formed homotrimer at some levels (Fig. 3B and Table 1). However, the mutants (M7, M9–M11) that have at least R227I induced cell death exhibiting EC_{50} of 48–65 ng/ml, which is only 2.4- to 3.5-fold lower level compared with that of wild-type TRAIL (Table 1). Analysis of cell morphology and detection of the cleavage of poly(ADP-ribose) polymerase (PARP) from its pro-forms by Western blotting confirmed that the mutants (M1–M4, M7, M9–M11) induced apoptotic cell death in HCT116 cells, like wild-type TRAIL (Supplementary Fig. S2) [4].

Conformational integrity around the zinc-binding site of $TRAIL_{C230A}$-derived mutants

We measured intrinsic Trp fluorescence of TRAIL mutants, comparing with wild-type TRAIL, to monitor effects of the mutations on the conformational integrity of the zinc-binding region [6]. TRAIL (residues 114–281) has two Trp residues, Trp154 and Trp231. Trp154 is positioned far away from the trimeric interface on the AA″ loop and partially exposed to solvent, whereas Trp231 close to the zinc-binding site is buried in the hydrophobic core constructed at the dimeric interface and hydrogen-bonded to the peptidyl oxygen of the EF loop of a neighboring monomer [5,6]. Thus discrepancy in Trp fluorescence among the mutants would be dominantly affected by the changes in apolar local environment of Trp231, partially reflecting the structural integrity of the zinc-binding site [6]. Wild-type TRAIL and its derived mutants showed Trp fluorescence with similar intensity at emission maximal wavelength of 330 nm (Fig. 4), consistent

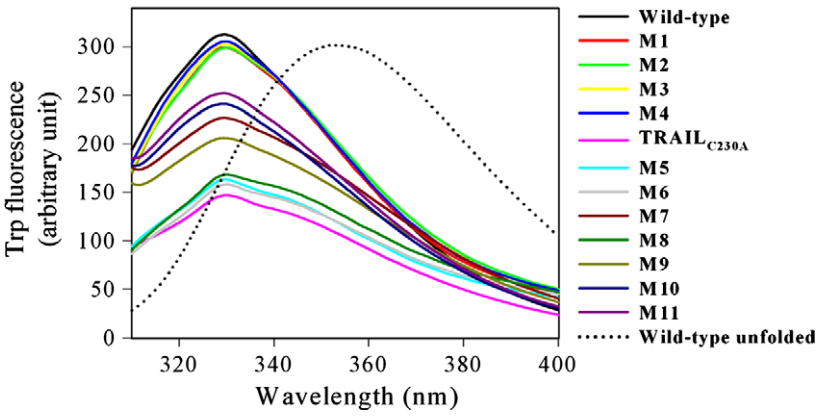

Fig. 4. Intrinsic tryptophan fluorescence emission spectra of wild-type TRAIL, $TRAIL_{C230A}$ and their mutants. Each protein (1 μM) was indicated in different colors. The spectra for wild-type TRAIL (1 μM) incubated with 6 M GdnHCl for 20 h at 25 °C was also shown in dotted line.

with the previous results [6]. $TRAIL_{C230A}$ exhibited significantly reduced Trp fluorescence down to 42% relative to that of wild-type TRAIL at the same maximum intensity wavelength (Fig. 4), consistent with the previous result [6]. Increased solvent accessibility leads to fluorescence quenching, resulting in decrease in fluorescence intensity [16]. The emission maximum wavelength of unfolded TRAIL by exposure to 6 M GdnHCl for 20 h was red shifted to ~350 nm (Fig. 4). Thus, the decreased fluorescence intensity of $TRAIL_{C230A}$ without changes in emission maximum wavelength reflected partial solvent exposure of Trp231 [6,16], which in turn indicates very flexible local structure around the zinc-binding region of zinc-free $TRAIL_{C230A}$ relative to the wild-type containing zinc ion.

For $TRAIL_{C230A}$-derived mutants, interestingly enough, the fluorescence intensity was increased in proportion to the homotrimerization level measured by SEC (Fig. 4 and Table 1). The mutants of M5 (Y183F), M6 (Y243F), and M8 (Y183F + Y243F) showed slightly increased intensity of the Trp fluorescence up to ~48% level of wild-type TRAIL. However, the mutants (M7, M9–M11) containing at least R227I displayed significant increases in the fluorescence intensity exhibiting M11 the highest intensity at ~80% level of wild-type TRAIL. This indicates that R227I mutation significantly induce rigid local structure around of the zinc-binding region of zinc-free $TRAIL_{C230A}$.

Discussion

$TRAIL_{C230A}$ exhibited only 4.4-fold lower affinity with TR2 than wild-type TRAIL, but it did not form a stable trimeric complex and exhibited no apoptotic activity, consistent with previous observations [6,9–11]. Alternative substitutions of Cys230 with Ser, Val, Ile, Met, Leu, Thr, or His gave the same results (data not shown). Promoting hydrophobic contacts by the three mutations of Y183F, Y243F, and R227I alone or in combinations at the trimeric interface of $TRAIL_{C230A}$ successfully induced the homotrimerization, the level of which varied depending on the mutations (Table 1). However, no direct correlationships between the induced homotrimerization level and apoptosis-inducing activity for the mutants were observed. Although $TRAIL_{C230A}$-derived mutants with Y183F (M5) and Y243F (M6) alone or together (M8) exhibited somewhat increased the homotrimerization level up to 41% of wild-type TRAIL, they did not show any biological activity even at the highest concentration (200 ng/ml, 24 h) tested (Table 1). In contrast, the mutants containing R227I (M7, M9–M11) exhibited significantly improved trimerization levels of more than 70% and only 2.4- to 3.5-fold lowered apoptosis-inducing activities in the TRAIL-sensitive cancer cells, compared with wild-type TRAIL (Table 1). Especially, M11, which has all the substitutions of Y183F, Y243F and R227I, showed ~80% homotrimerizaiton level and only ~2.4-fold lowered apoptosis-inducing activity, compared with wild-type TRAIL (Table 1). These results suggest that the homotrimeric state induced by R227I, but not by Y183F and/or Y243F, is critical for triggering apoptosis-inducing signal by $TRAIL_{C230A}$.

The residues between 231 and 236 in the EF loop located around the zinc-binding site near the tip of wedge-shaped homotrimer are disordered in the zinc-depleted TRAIL structure [5], but visualized in the crystal structure containing the zinc ion [6,15], suggesting that the zinc-coordination is critical for maintaining rigid conformational stability of the loop. In other words, without the zinc-coordination, the EF loop is flexible enough to be readily exposed to the solvent, which explains significant decreases in the Trp231 fluorescence intensity for zinc-depleted TRAIL [6] and $TRAIL_{C230A}$ (Fig. 4). As aforementioned, the positive side chains of Arg227 located at right upper the zinc-binding site (Fig. 1C) are surrounded with very hydrophobic environment, which might invoke repulsive electrostatic interactions between them [6,14]. The probable repulsive forces by Arg227 residues seem to delocalize the following EF loop region to be disordered and eventually destabilize the trimeric state of TRAIL, unless they were held together by the near zinc-coordination with the three Cys230 residues. Our results demonstrated that R227I mutation, removing the possible repulsive interactions among Arg227 and promoting hydrophobicity there, significantly induced homotrimerization and rigid local structures of EF loop around the zinc-binding region in zinc-free $TRAIL_{C230A}$ (Fig. 4). These results suggest that the loss of conformational rigidity of the zinc-binding region due to unfavorable electrostatic repulsion by Arg227 is responsible for the negligible homotrimerization of zinc-depleted or Cys230-substituted TRAIL.

The importance of ordered, rigid structure around the zinc-binding sites for the bioactivity of TRAIL was also demonstrated by zinc-depleted or Cys230-substituted TRAIL, which showed the complete loss of bioactivity [5,6,9–11]. The geometry of the tetrahedral zinc-binding site in TRAIL alone is identical with that of the TR2-TRAIL complex, and the buried zinc ion does not interact with the receptor [6,15]. However, the TR2-TRAIL complex structure showed that several residues of Gln205, Glu236, and Tyr237 residues in so called 'patch A' region directly interact with TR2 and simultaneously are hydrogen-bonded to the Cys230 containing loop [7,8,15], suggesting that the local conformation around the zinc-binding site can affect the complex formation and, hence, the biological activity. Interestingly, single Ala substitutions of Glu205, Glu236, and Tyr237 of TRAIL resulted in more than 5-fold decreased affinity with TR2 and 10-fold reduction in the bioactivity [6]. The defined, rigid complex formation between TRAIL and its death-inducing receptors, which in turn dictates a precise positioning of the three transmembrane helices and subsequently intracellular death domain of the receptors, will be essential for the efficient triggering the apoptotic signal [8]. The disordered, flexible structure around the zinc-binding region of zinc-free $TRAIL_{C230A}$ might not induce the rigid complex with the receptors, leading to significant or complete loss of the

biological activity. However, induction of the ordered, rigid structure of the region by R227I mutation in $TRAIL_{C230A}$, as evidenced by significantly increased intensity of Trp231 fluorescence, recovered the biological activity (Figs. 3 and 4). Taken together, our results suggest that the ordered, rigid local structure around the zinc-binding site at the tip of wedge-shaped homotrimer is critical for the homotrimerization and biological activity of TRAIL.

Acknowledgments

This work was supported by grants from Korea Research Foundation (205-2004-D00068 to Y.S.K.), the National R&D Program for Cancer Control, Ministry of Health & Welfare (0520110-1 to Y.S.K.), and the "GRRC" Project of Gyeonggi Provincial Government (to Y.S.K. and M.H.K.), Republic of Korea.

Appendix A. Supplementary data

Supplementary data associated with this article can be found, in the online version, at doi:10.1016/j.bbrc.2007.08.075.

References

[1] A. Ashkenazi, Targeting death and decoy receptors of the tumour-necrosis factor superfamily, Nat. Rev. Cancer 2 (2002) 420–430.
[2] E.W. Duiker, C.H. Mom, S. de Jong, P.H. Willemse, J.A. Gietema, A.G. van der Zee, E.G. de Vries, The clinical trail of TRAIL, Eur. J. Cancer 42 (2006) 2233–2240.
[3] A. Ashkenazi, R.C. Pai, S. Fong, S. Leung, D.A. Lawrence, S.A. Marsters, C. Blackie, L. Chang, A.E. McMurtrey, A. Hebert, L. DeForge, I.L. Koumenis, D. Lewis, L. Harris, J. Bussiere, H. Koeppen, Z. Shahrokh, R.H. Schwall, Safety and antitumor activity of recombinant soluble Apo2 ligand, J. Clin. Invest. 104 (1999) 155–162.
[4] K.J. Park, S.H. Lee, T.I. Kim, H.W. Lee, C.H. Lee, E.H. Kim, J.Y. Jang, K.S. Choi, M.H. Kwon, Y.S. Kim, A human scFv antibody against TRAIL receptor 2 induces autophagic cell death in both TRAIL-sensitive and TRAIL-resistant cancer cells, Cancer Res. 67 (2007) 7327–7334.
[5] S.S. Cha, M.S. Kim, Y.H. Choi, B.J. Sung, N.K. Shin, H.C. Shin, Y.C. Sung, B.H. Oh, 2.8 A resolution crystal structure of human TRAIL, a cytokine with selective antitumor activity, Immunity 11 (1999) 253–261.
[6] S.G. Hymowitz, M.P. O'Connell, M.H. Ultsch, A. Hurst, K. Totpal, A. Ashkenazi, A.M. de Vos, R.F. Kelley, A unique zinc-binding site revealed by a high-resolution X-ray structure of homotrimeric Apo2L/TRAIL, Biochemistry 39 (2000) 633–640.
[7] S.S. Cha, B.J. Sung, Y.A. Kim, Y.L. Song, H.J. Kim, S. Kim, M.S. Lee, B.H. Oh, Crystal structure of TRAIL-DR5 complex identifies a critical role of the unique frame insertion in conferring recognition specificity, J. Biol. Chem. 275 (2000) 31171–31177.
[8] J. Mongkolsapaya, J.M. Grimes, N. Chen, X.N. Xu, D.I. Stuart, E.Y. Jones, G.R. Screaton, Structure of the TRAIL-DR5 complex reveals mechanisms conferring specificity in apoptotic initiation, Nat. Struct. Biol. 6 (1999) 1048–1053.
[9] J.L. Bodmer, P. Meier, J. Tschopp, P. Schneider, Cysteine 230 is essential for the structure and activity of the cytotoxic ligand TRAIL, J. Biol. Chem. 275 (2000) 20632–20637.
[10] D.W. Seol, T.R. Billiar, Cysteine 230 modulates tumor necrosis factor-related apoptosis-inducing ligand activity, Cancer Res. 60 (2000) 3152–3154.
[11] D. Trabzuni, K.S. Famulski, M. Ahmad, Functional analysis of tumour necrosis factor-alpha-related apoptosis-inducing ligand (TRAIL): cysteine-230 plays a critical role in the homotrimerization and biological activity of this novel tumoricidal cytokine, Biochem. J. 350 (Pt 2) (2000) 505–510.
[12] H.W. Lee, S.H. Lee, Y.W. Ryu, M.H. Kwon, Y.S. Kim, Homomeric and heteromeric interactions of the extracellular domains of death receptors and death decoy receptors, Biochem. Biophys. Res. Commun. 330 (2005) 1205–1212.
[13] Y.R. Kim, J.S. Kim, S.H. Lee, W.R. Lee, J.N. Sohn, Y.C. Chung, H.K. Shim, S.C. Lee, M.H. Kwon, Y.S. Kim, Heavy and light chain variable single domains of an anti-DNA binding antibody hydrolyze both double- and single-stranded DNAs without sequence specificity, J. Biol. Chem. 281 (2006) 15287–15295.
[14] A.M. van der Sloot, M.M. Mullally, G. Fernandez-Ballester, L. Serrano, W.J. Quax, Stabilization of TRAIL, an all-beta-sheet multimeric protein, using computational redesign, Protein Eng. Des. Sel. 17 (2004) 673–680.
[15] S.G. Hymowitz, H.W. Christinger, G. Fuh, M. Ultsch, M. O'Connell, R.F. Kelley, A. Ashkenazi, A.M. de Vos, Triggering cell death: the crystal structure of Apo2L/TRAIL in a complex with death receptor 5, Mol. Cell 4 (1999) 563–571.
[16] J.R. Lakowicz, Principles of fluorescence spectroscopy, second ed., Kluwer Academic/Plenum Publishers, New York, 1999.